Exposing mass structure in gravitational lenses at milli-arcsecond resolution

Devon Powell

15 June 2022

News from the Dark 7

Collaborators:
Simona Vegetti (MPA), Hannah Stacey (MPA), John McKean (Groningen),
Cristiana Spingola (Bologna), Francesca Rizzo (DAWN/Neils Bohr Inst.)

Publications:

Powell et al., "A lensed radio jet at milli-arcsecond resolution", *In prep.*, 2022.

Powell et al., "A novel approach to visibility-space modelling of interferometric gravitational lens observations at high angular resolution", *MNRAS*, 2021.

Science with strong lenses

- **Studies of the mass distribution in the lens (for example, dark matter substructure detection)**

  e.g. Ritondale et al. (2019), Despali et al. (2018), Birrer et al. (2017), Hezaveh et al. (2016), Vegetti et al. (2014), Vegetti et al. (2012), Vegetti et al. (2010)

- Source science taking advantage of magnification

  e.g. Spingola et al. (2019), Rizzo et al. (2018), Johnson et al. (2017), Leethochawalit et al. (2016), Swinbank et al. (2015)

- Cosmology using time delays between images

  e.g. Rusu et al. (2019), Suyu et al. (2018), Wong et al. (2017), Treu and Marshall (2016), Chen et al. (2016), Courbin et al. (2011), Fassnacht et al. (2002)

- Polarimetry and rotation measure synthesis

  e.g. Simon Ndiritu, Mao et al. (2017)

Lots of science with lenses - review in Koopmans et al. (2009).

Low-Mass Perturbers (LoMPs) with lensing

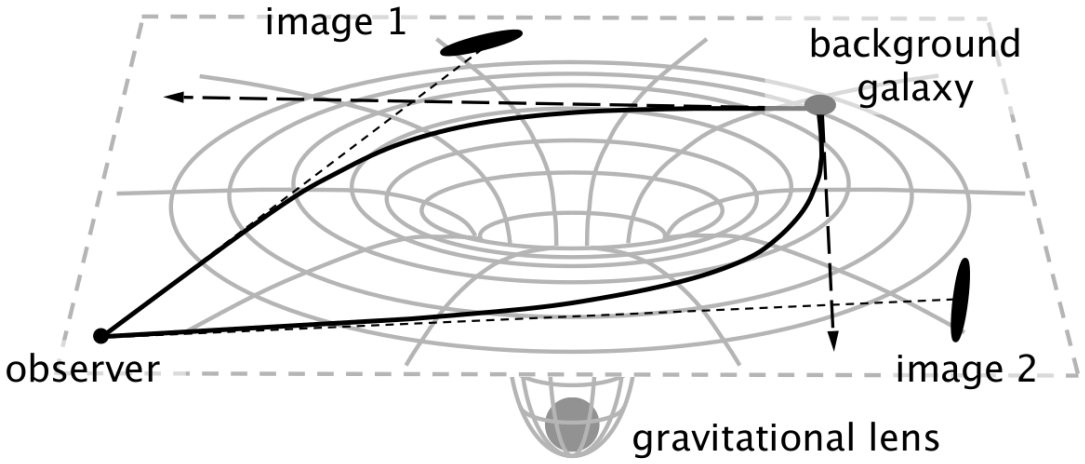

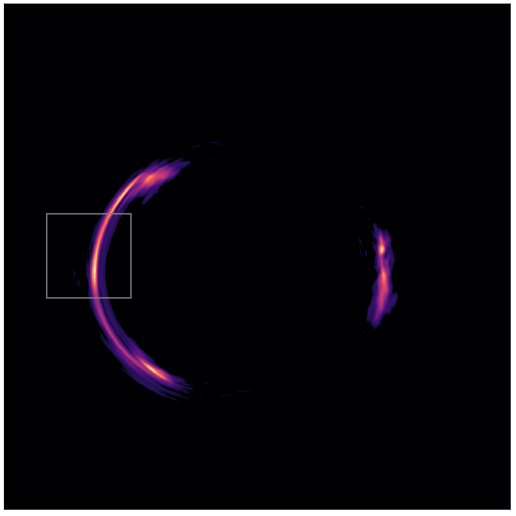

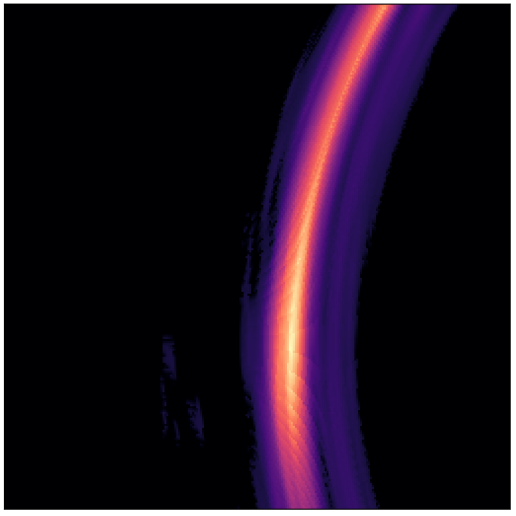

Low-Mass Perturbers (LoMPs) with lensing

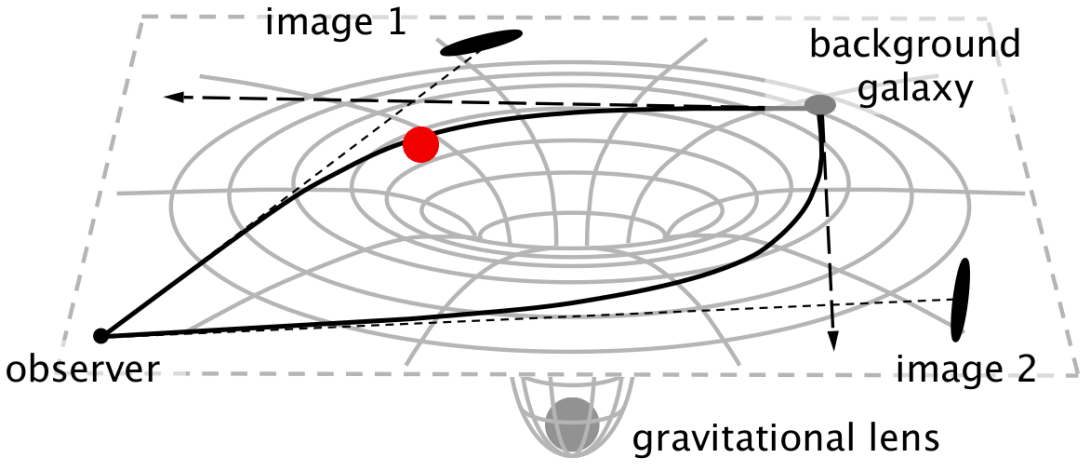

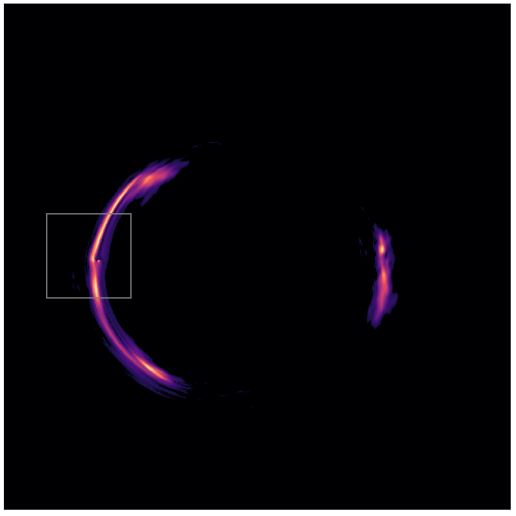

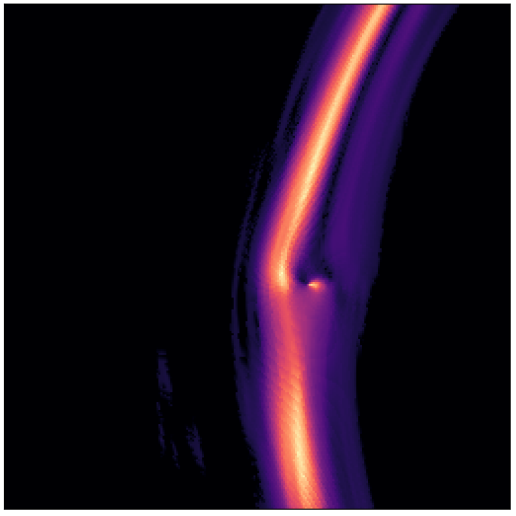

Example: JVAS B1938+666

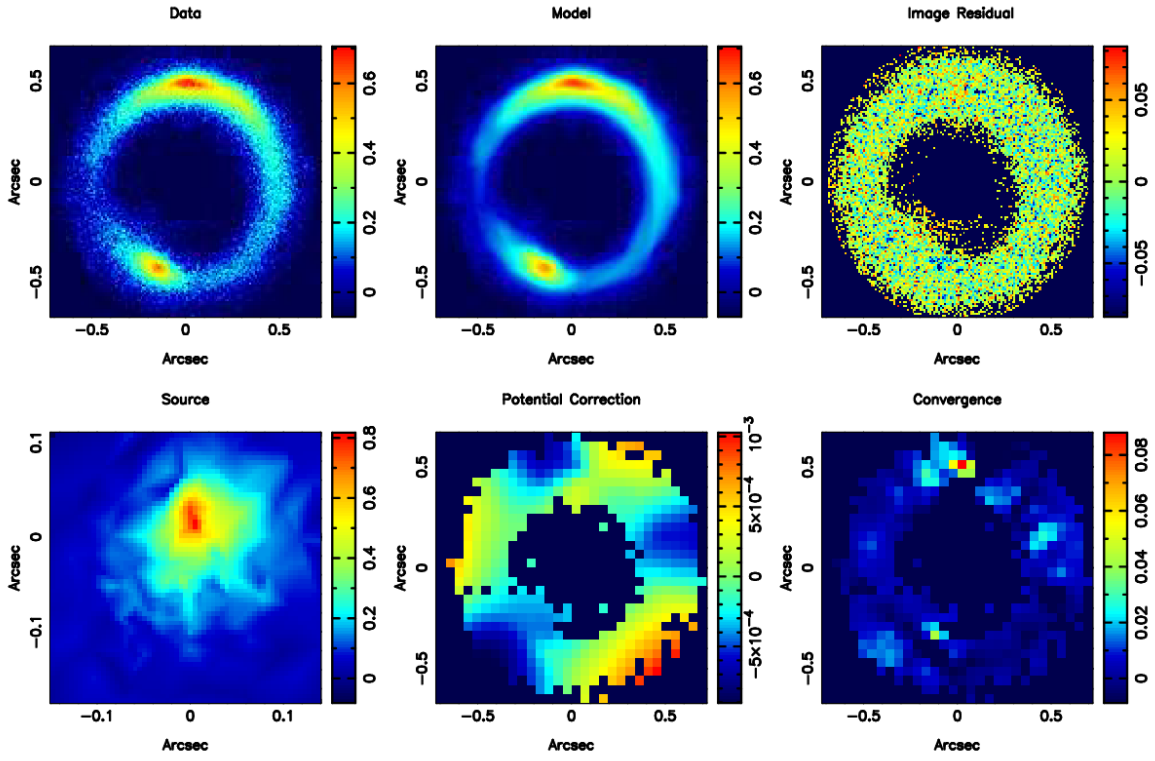

- Substructure detection using gravitational imaging by Vegetti et al. (2012).
- Mass is a few $\times 10^8\ M_\odot$.
- Observed with Keck adaptive optics, PSF $\sim$ 70 mas.

Mass function: CDM vs. WDM

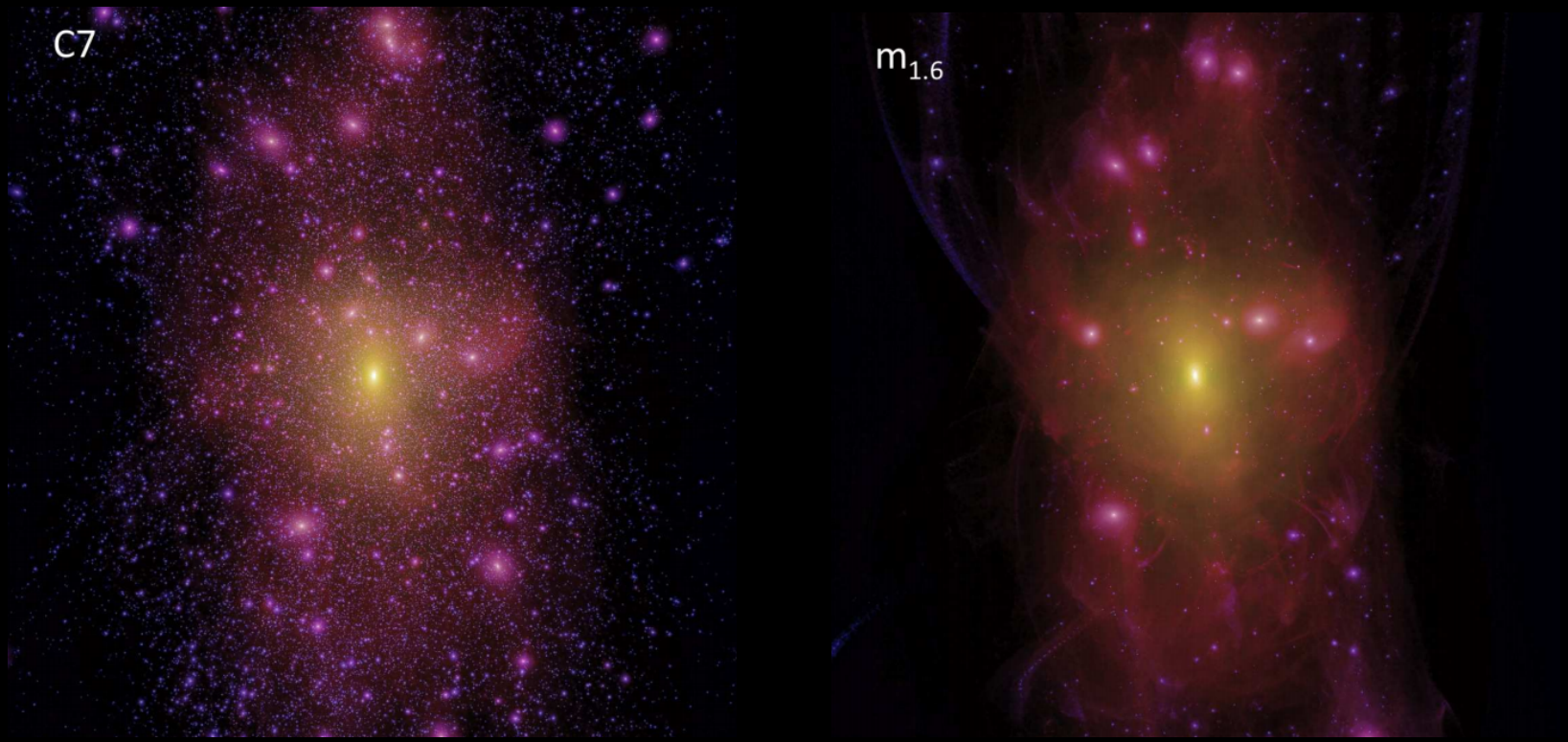

Lovell et al. (2014)

Mass function: CDM vs. WDM

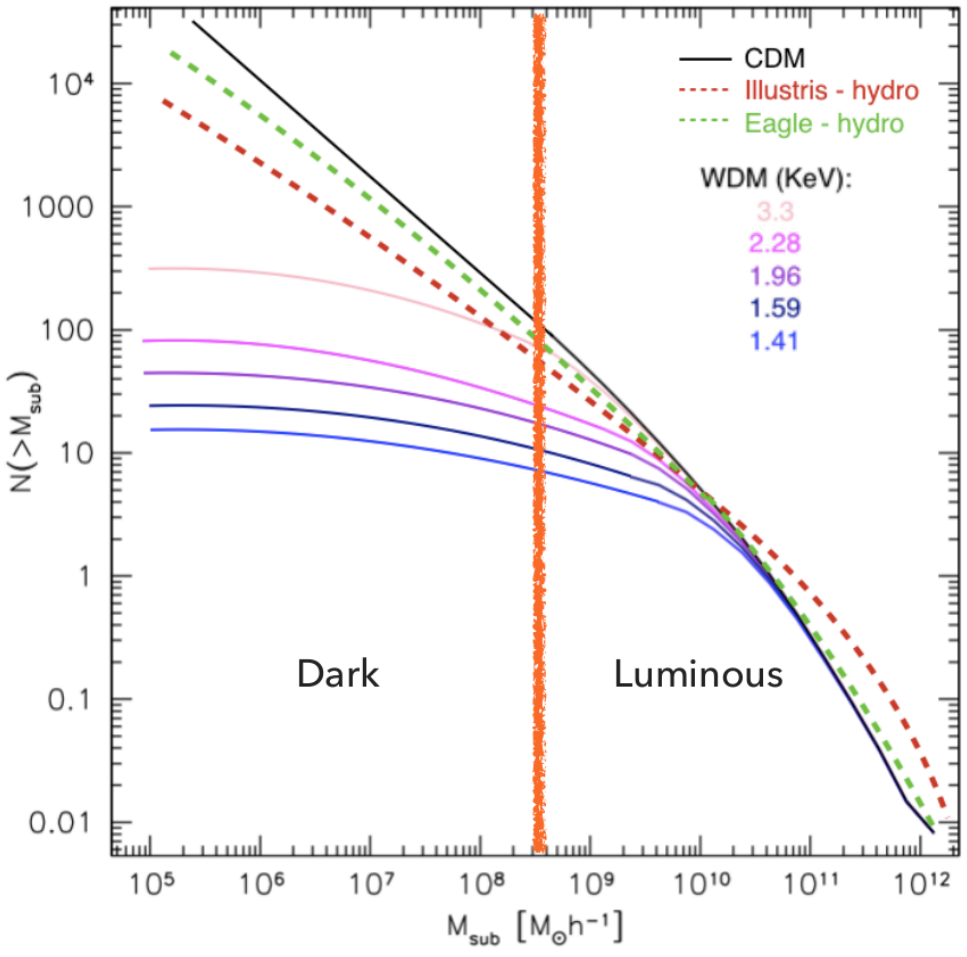

Despali and Vegetti (2017), Lovell et al. (2014)

Angular resolution

- Sensitivity to low-mass haloes is limited by angular resolution
- Roughly speaking, the resolution must be better than the scale radius of the perturber.

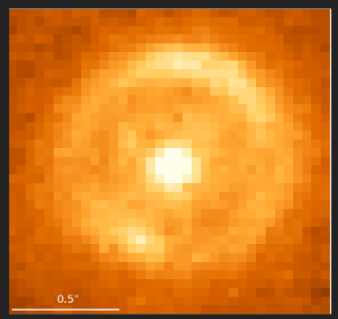

HST

10^9 M_{sun}

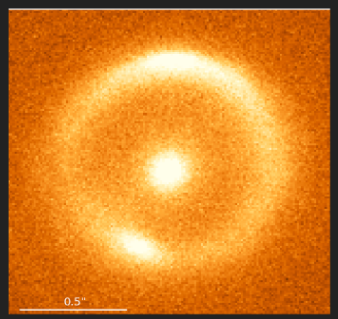

Keck AO

10^8 M_{sun}

>2024

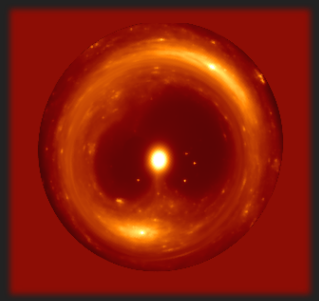

E-ELT

10^7-10^6 M_{sun}

NOW

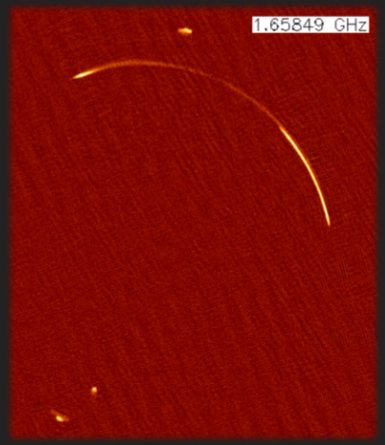

GVLBI

10^6 M_{sun}

Angular resolution

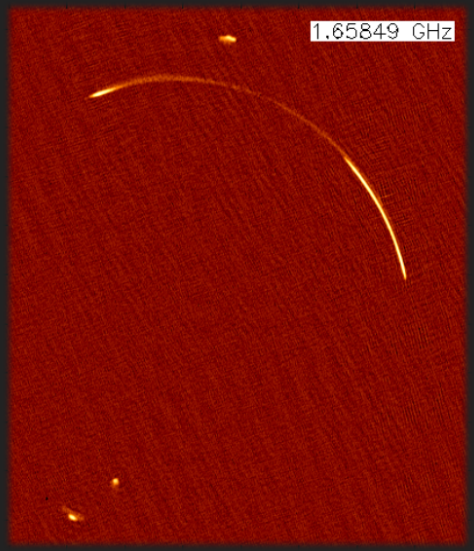

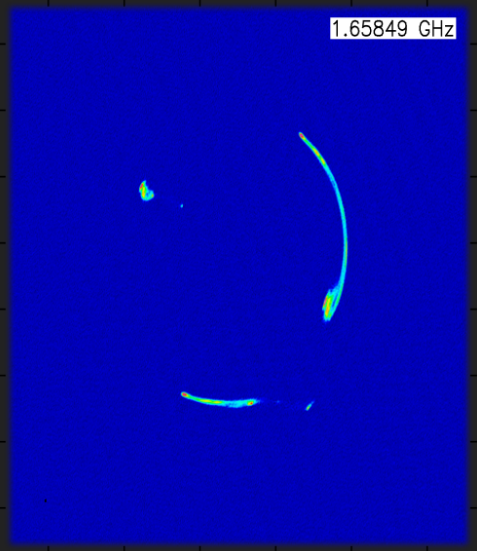

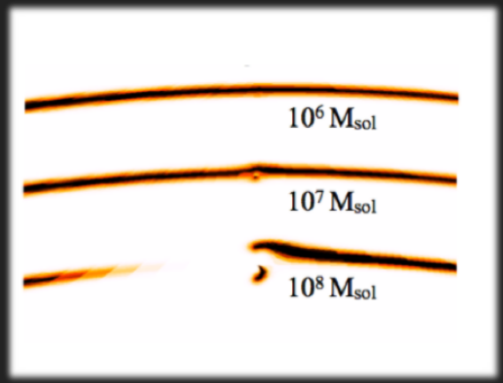

For 10 lenses, number of detectable objects:

CDM ~ 30

WDM (3.3 keV) ~ 0.9

Vegetti

GVLBI and lens modeling

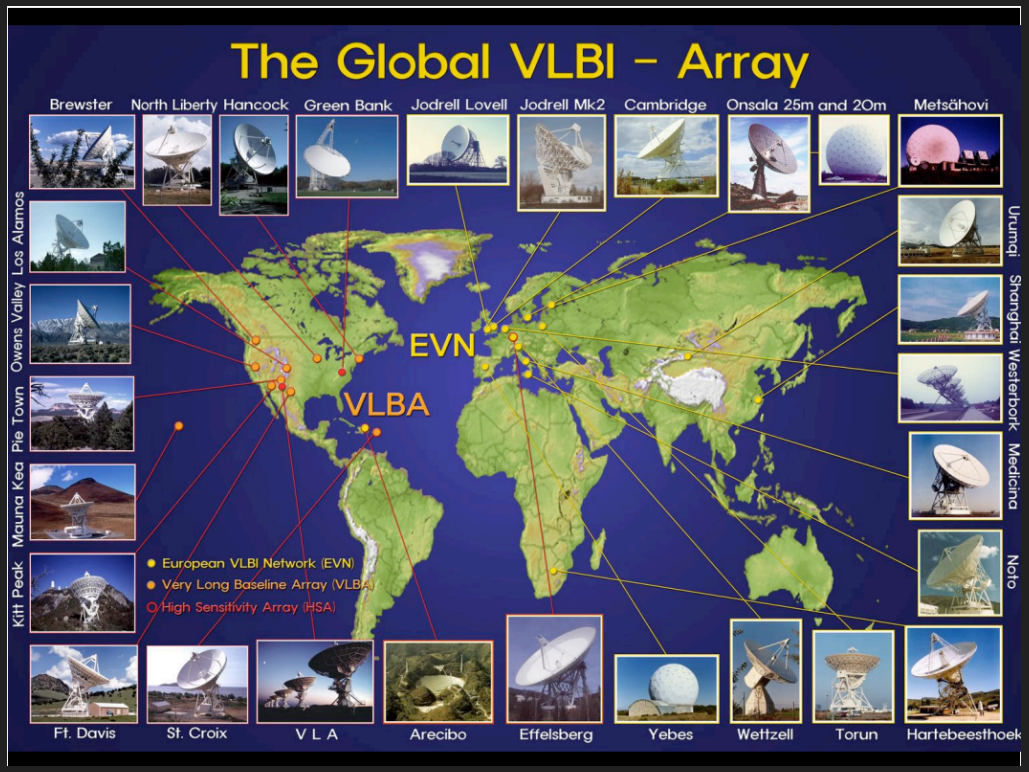

- GVLBI array (Global Very Long Baseline Interferometry)
- Sub-milliarcsec resolution at shorter wavelengths
- Large numbers of visibilities (can be $\mathcal{O}(10^{10})$) pose a challenge for modelling.

MG J0751+2716

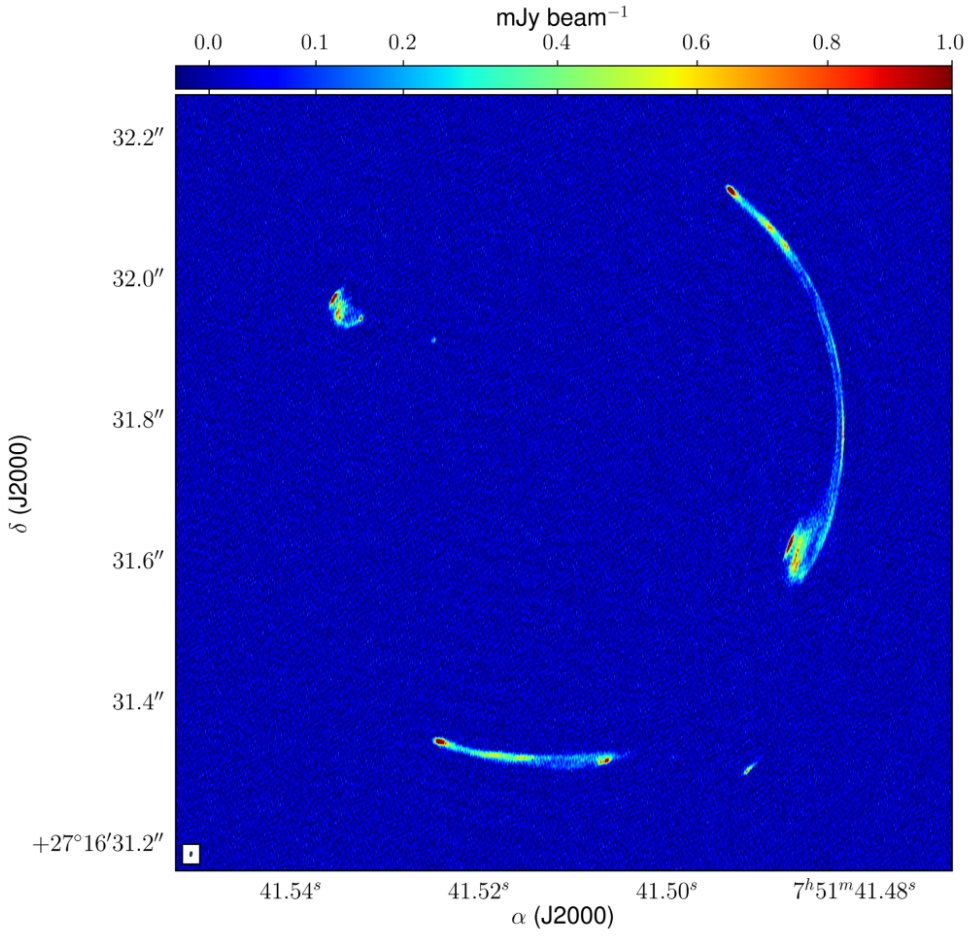

- Lensed radio jet, observed with global VLBI (PI: McKean)
- Extended, thin arcs ideal for detecting structure in the lens
- Spingola et al. (2018) fits image positions to within a few mas using a power-law ellipsoid lens model.

Forward modeling

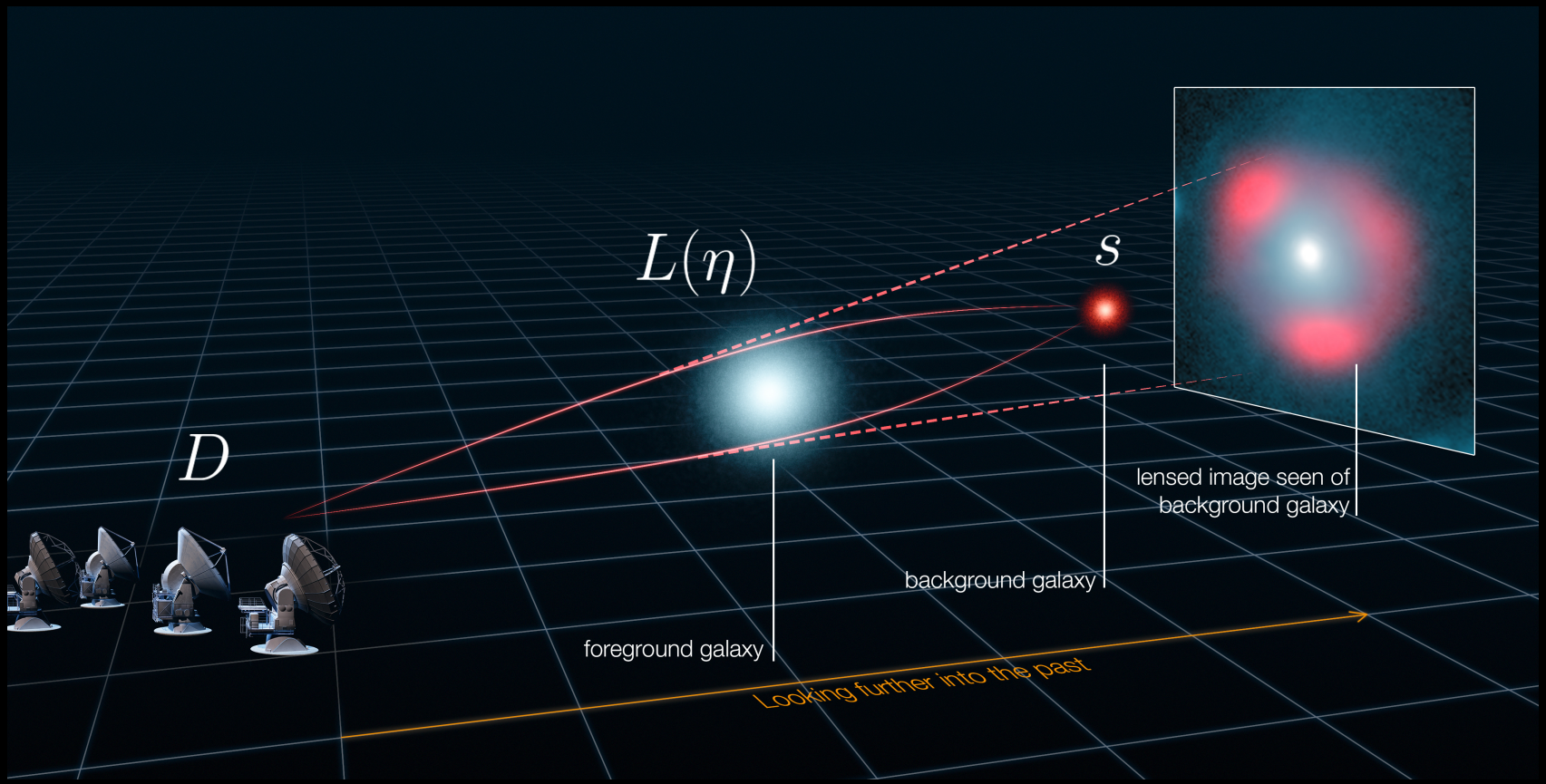

ALMA (ESO/NRAO/NAOJ), L. Calada (ESO), Y. Hezaveh et al.

Computational challenges

The log-posterior is:

$$2 \log P(\eta_H, \lambda \mid \mathbf{d}) = -\chi^2 - s_{\mathrm{MP}}{}^T R s_{\mathrm{MP}} - \log\det \Sigma_s^{-1}$$
$$+ \log \lambda + \log\det R - N \log 2\pi - \log\det C_d$$

- Pixellated source s_{MP} is expensive (solved using CG)
- χ^2 is expensive (dimension N_{vis}). We have a nice trick for it.
- Σ_s^{-1} is the solution matrix for the source inversion.
  It does not exist explicitly as a matrix (contains FFTs).
- We must compute s_{MP}, χ^2, and $\log\det \Sigma_s^{-1}$.
- New numerical methods, implemented on MPI+GPUs, let us do this efficiently (Powell et al., 2021).

MG J0751+2716 data

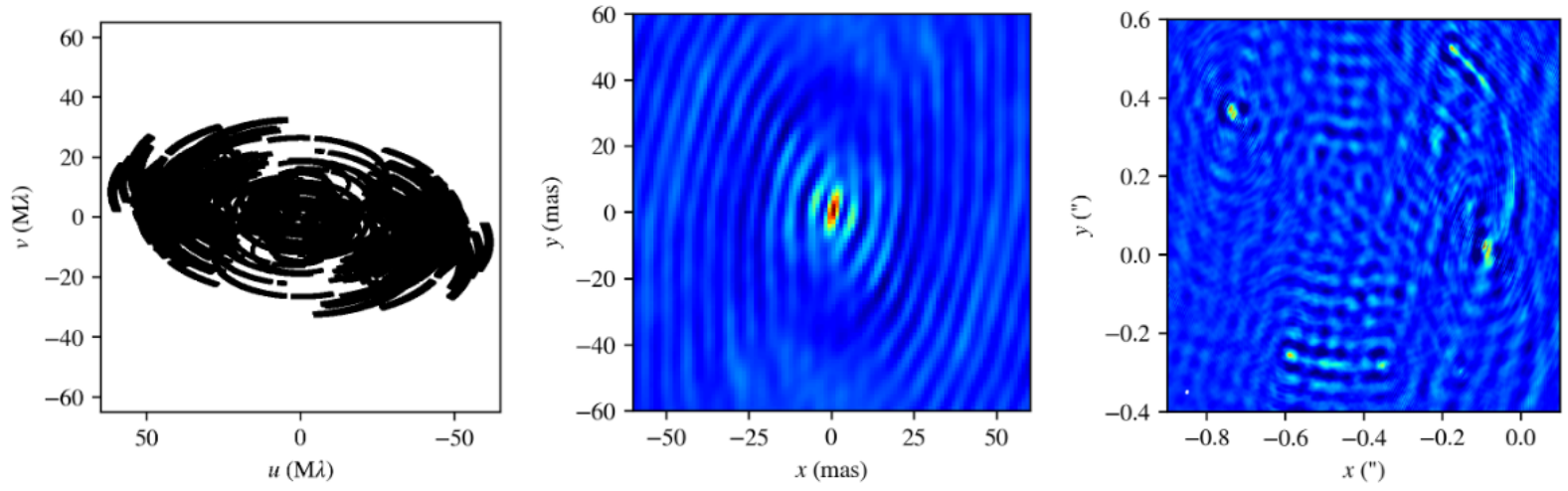

Figure 1. uv-coverage (left), naturally-weighted dirty beam (center), and dirty image (right) of the global VLBI observation of MG J0751+2716 . The main lobe of the dirty beam is 5.5×1.8 mas^2 (FWHM) with a position angle of 9.8 degrees. The (x, y) coordinates of the dirty image are given in arcseconds relative to the phase center. The beam ellipse is shown in white in the lower-left corner of the dirty image.

- $\sim$ 5 milli-arcsecond resolution at 1.65 GHz
- 2.5×10^8 visibilities
- We fit in visibility space without averaging

Test on mock data

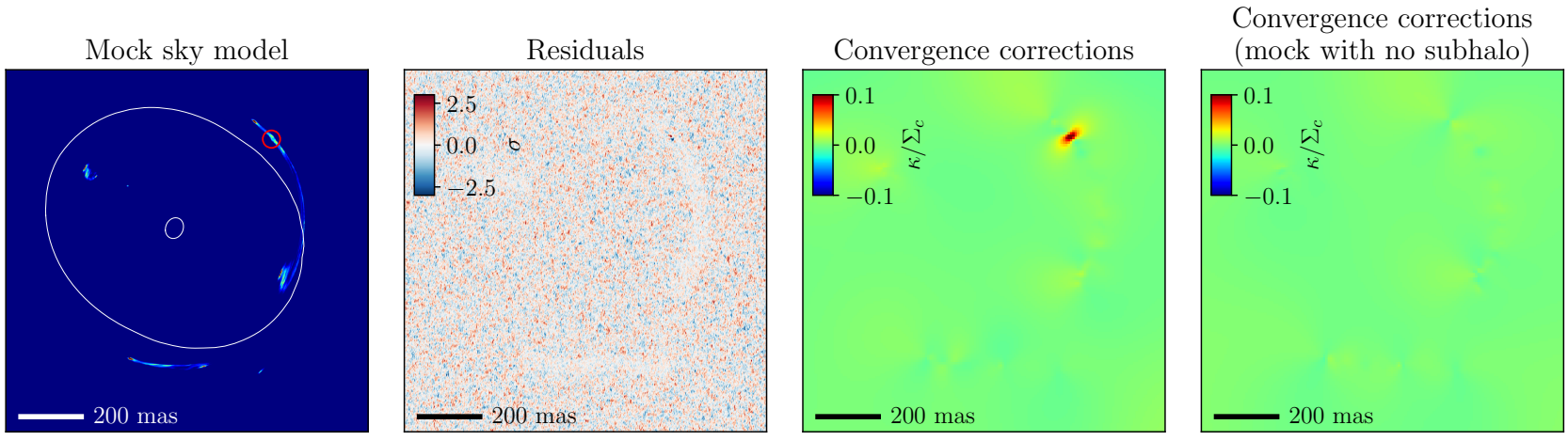

- Mock data duplicates SNR and *uv*-coverage.
- Source model is as close as we can reasonably come to the truth, without a-priori knowledge.
- 10^7 $M_\odot$ substructure is clearly detected.

Lens models summary

H	Description
PL	Power-law ellipsoid (PEMD)
PL+FG	PEMD plus field galaxies
PL+M4	PEMD plus multipoles $m \leq 4$
PL+PX	PL plus potential corrections
PL+FG+PX	PL+FG plus potential corrections
PL+M4+PX	PL+M4 plus potential corrections

PL:

$$\kappa(x, y) = \frac{\kappa_0 \left(2 - \frac{\gamma}{2}\right) q^{\gamma - \frac{3}{2}}}{2 \left[q^2 x^2 + y^2\right]^{\frac{\gamma - 1}{2}}}$$

PL+M4:

$$\kappa_m(r, \theta) = r^{-(\gamma-1)} \left[a_m \sin(m\theta) + b_m \cos(m\theta)\right]$$

PL+FG:

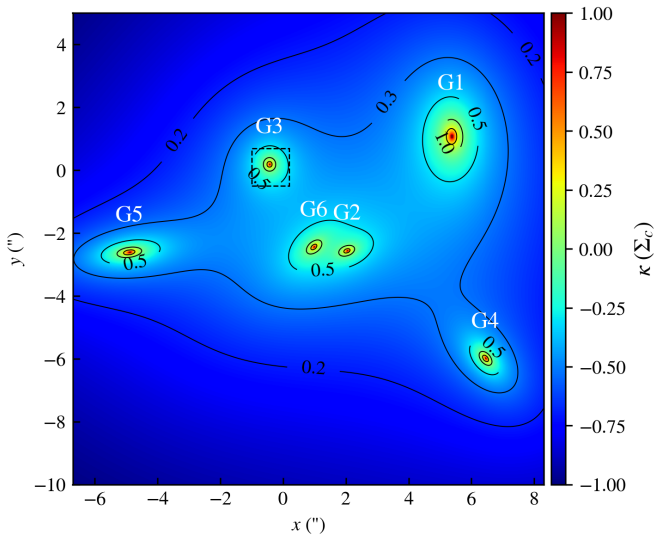

MAP model comparison (visual)

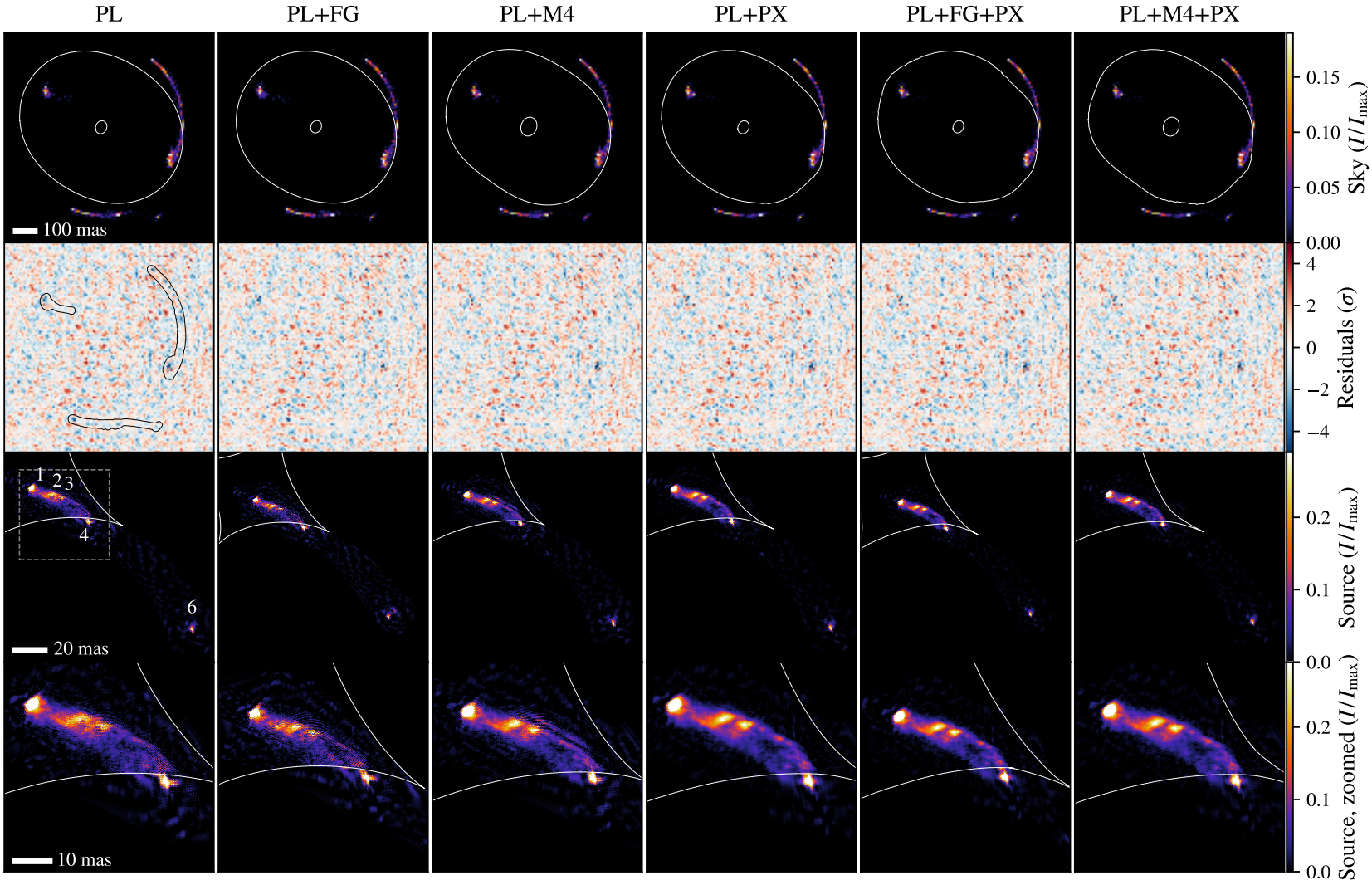

MAP model comparison (visual)

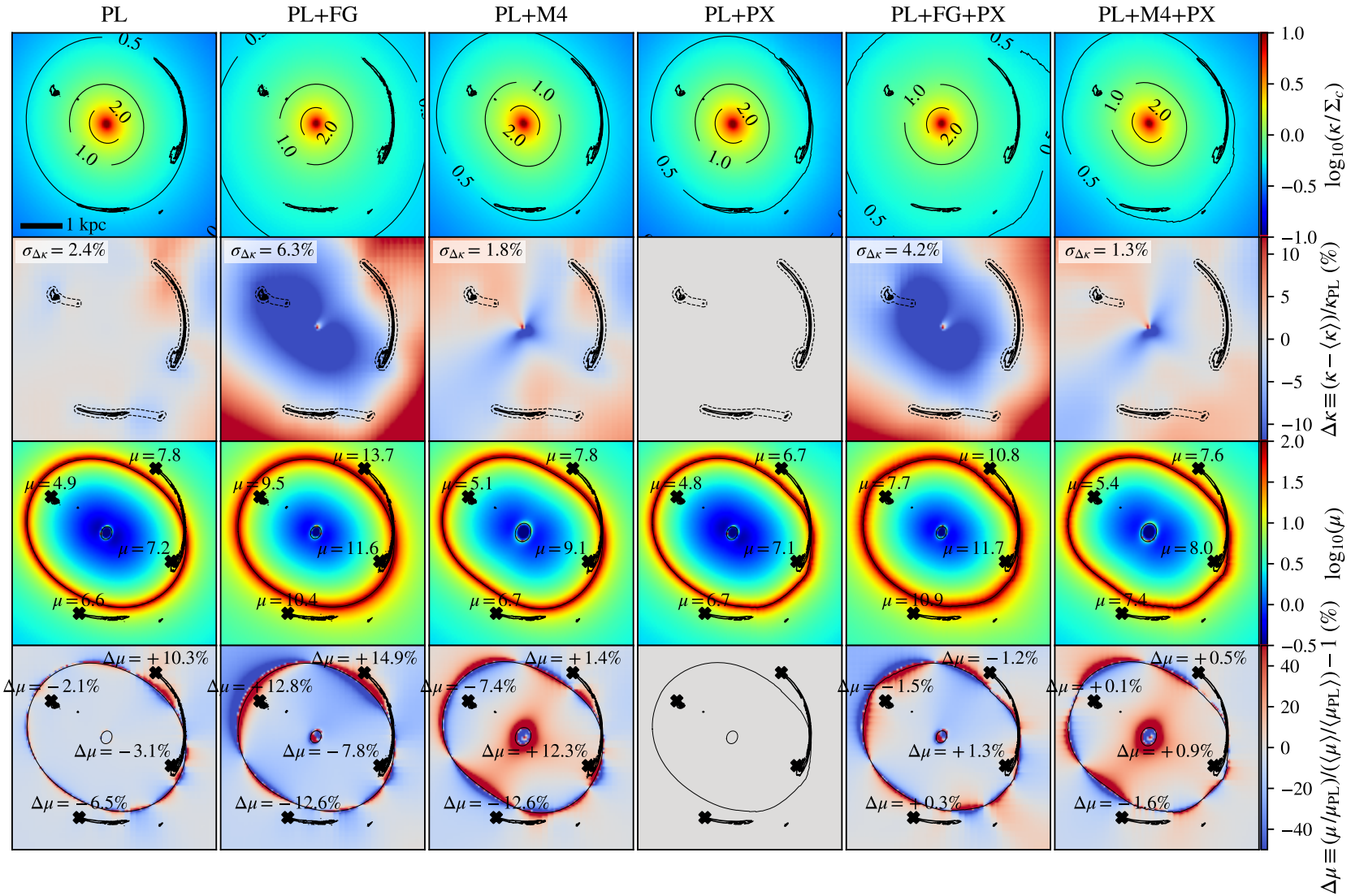

MAP model comparison (objective)

H	Description	$\Delta \log \mathcal{E}_{\rm H}$	$\Delta \log P_{\rm H}$	$\sigma_{\Delta\kappa}$ (%)	f_{H_0} (%)	$\lvert\Delta\mu\rvert_{\rm max}$ (%)
PL	Power-law ellipsoid (PEMD)	$\equiv \mathbf{0}$	-	2.4	+0.6	10.3
PL+FG	PEMD plus field galaxies	$\mathbf{-7060}$	-	6.3	−22.4	14.9
PL+M4	PEMD plus multipoles $m \leq 4$	$\mathbf{+4751}$	-	1.8	−6.2	12.6
PL+PX	PL plus potential corrections	-	$\equiv \mathbf{0}$	$\equiv 0$	$\equiv 0$	$\equiv 0$
PL+FG+PX	PL+FG plus potential corrections	-	$\mathbf{-1084}$	4.2	−24.8	1.2
PL+M4+PX	PL+M4 plus potential corrections	-	$\mathbf{-21}$	1.3	−6.6	1.6

Table 1: Summary of the main quantitative results from this work. For each parametric lens model parameterization, we present the Bayes factor $\Delta \log \mathcal{E}_{\rm H}$ relative to the fiducial model PL. For models which include pixellated potential corrections (PX), we present the maximum log-posterior $\Delta \log P_{\rm H}$ relative to PL+PX. The next column contains the RMS fractional difference in convergence $\sigma_{\Delta\kappa}$ relative to the best model PL+PX, measured inside a masked region within 17 mas (3 beam widths) of the lensed images (see Figure 1). We also show a comparison of the fractional difference f_{H_0} in a measurement of H_0 which would be inferred using time-delay cosmography under each model (with PL+PX as the "truth"). The last column contains the maximum change in flux for the brightest part of the source (source component "1"; see Figures 1, 2, and 3) in each model, standardized to the flux-weighted mean magnification. Although the projected surface mass densities depart from the best PL+PX profile by only a few per cent (RMS) within the mask, the effect on inferences made using time-delays or flux ratios can be substantial.

MG J0751+2716 (best lens model PL+PX)

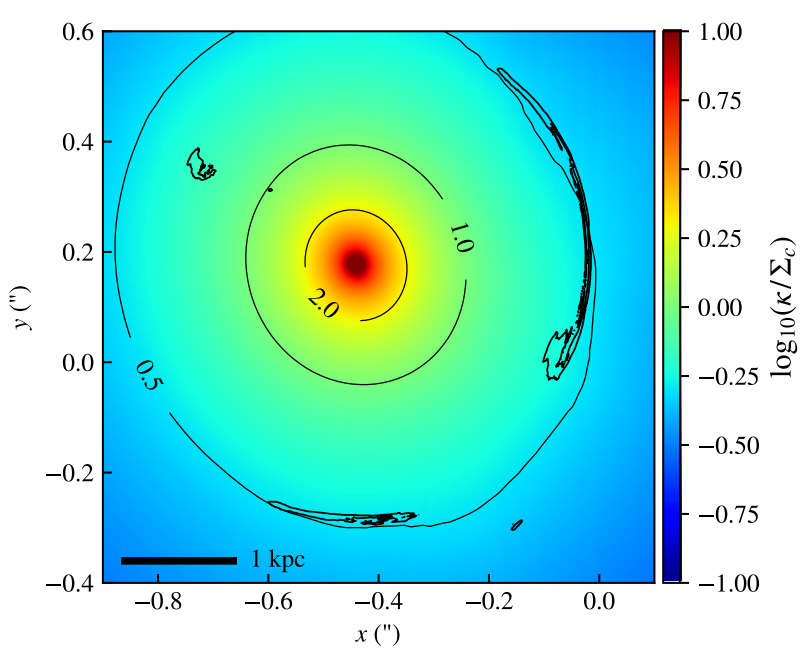

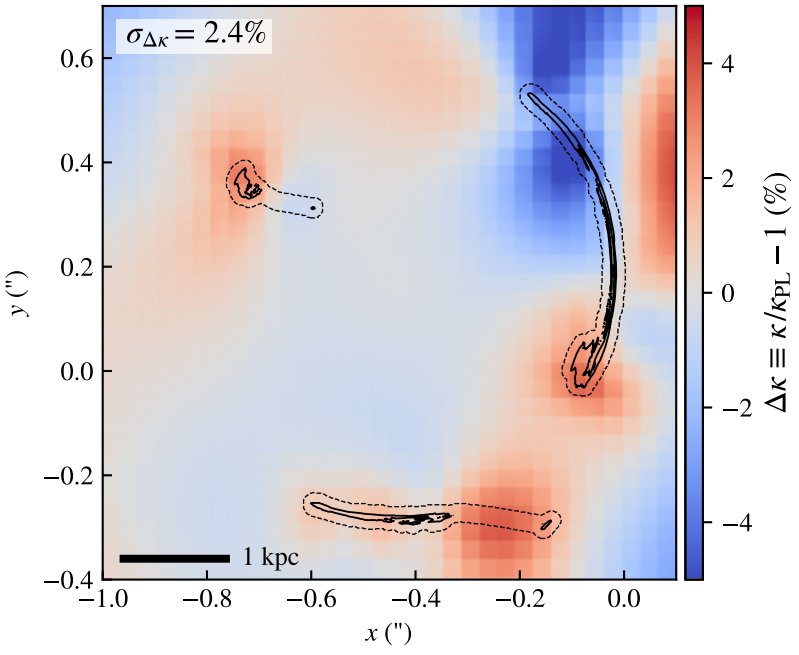

- Relatively low-level (2.4%) corrections to elliptical power-law focus the source.
- Flux ratios improve by around 10%.

MG J0751+2716 (best lens model PL+PX)

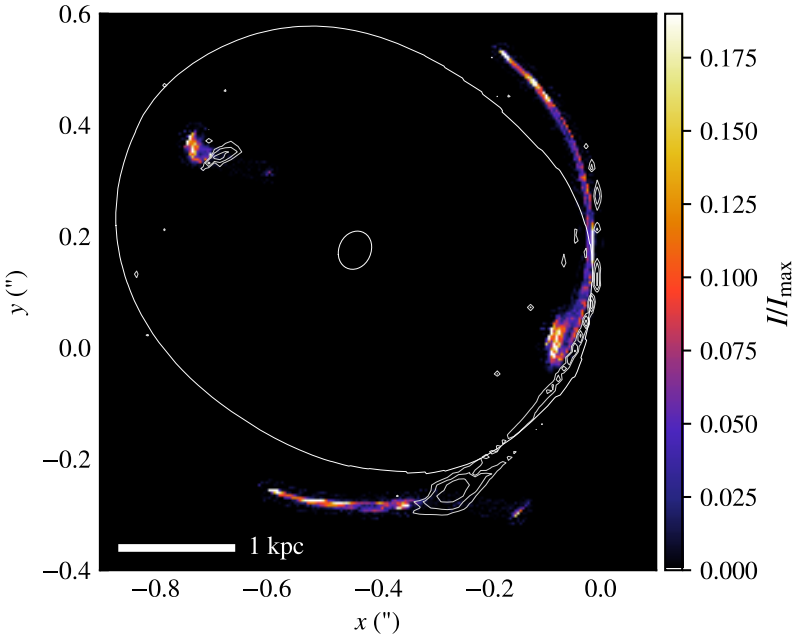

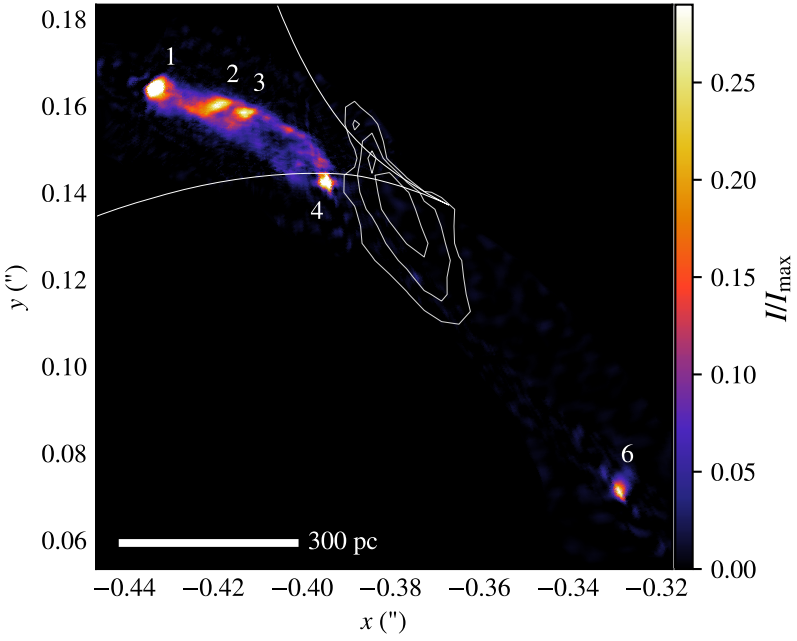

- This image from 2.5×10^8 visibilities, with no averaging
- Single posterior evaluation (source inversion + χ^2 evaluation) in < 1 minute on 1 core + 1 GPU (!)
- White contours are Keck AO optical data
- *Source is very well-focused already. What about substructure?*

But what about the priors???

Data:

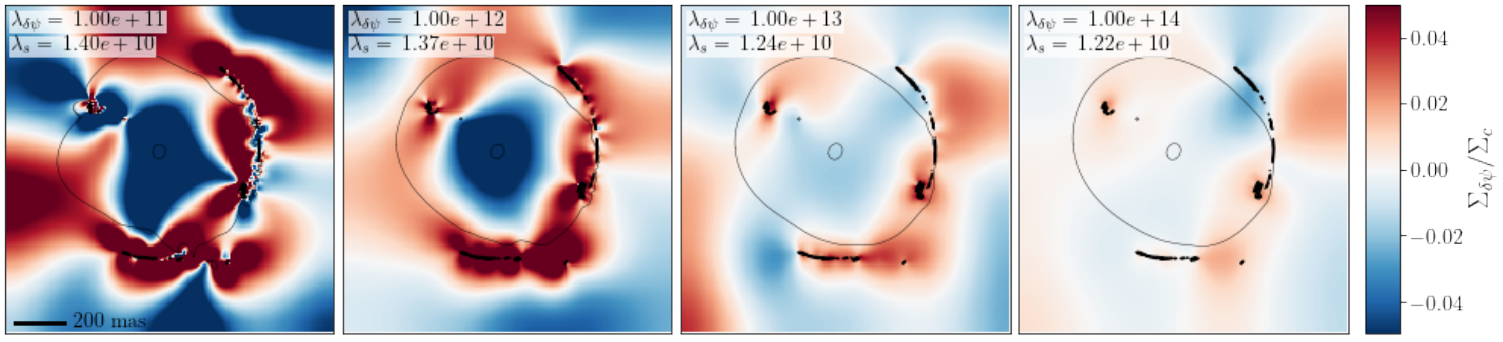

Mock:

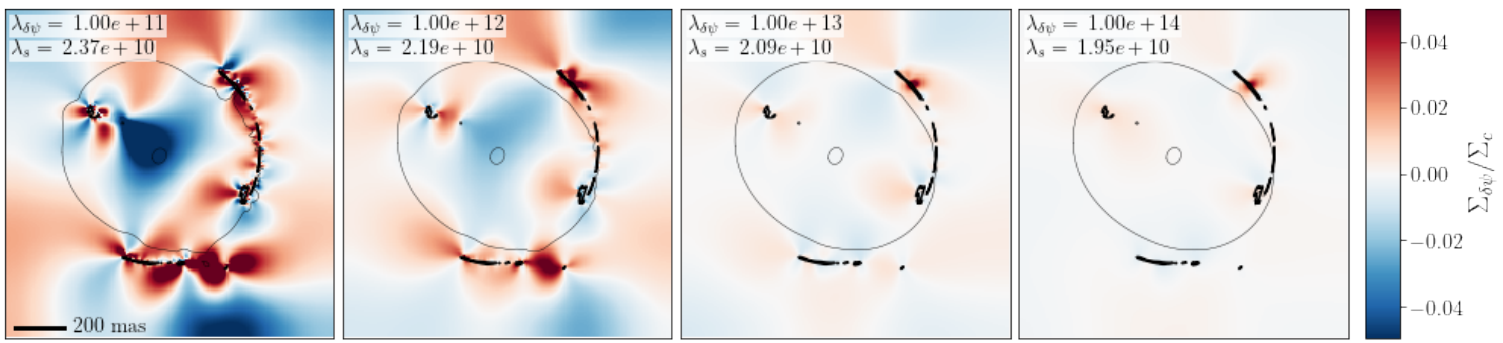

- Structure of the potential corrections is dependent on the prior!
- What about a population of substructures? Moving into statistical regime, rather than individual detections.

Conclusions

- First image of a lensed radio jet!
- Source structure allows us to "image" the lens surface density.
- A *lot* of computational challenges overcome to this point.
- Still, much work to do in understanding the priors, avoiding over-fitting, etc...
- Collaborators (Cristiana Spingola, Di Wen) are working on doing this analysis for other VLBI lenses (MG2016, B1938...)
- Future work: Warm DM and Fuzzy DM using adaptive Bayesian computation (ABC).
- Future work: Joint optical/radio modeling.
- Future work: Built-in self-calibration of visibility phases and amplitudes.

Sneak preview: Fuzzy DM

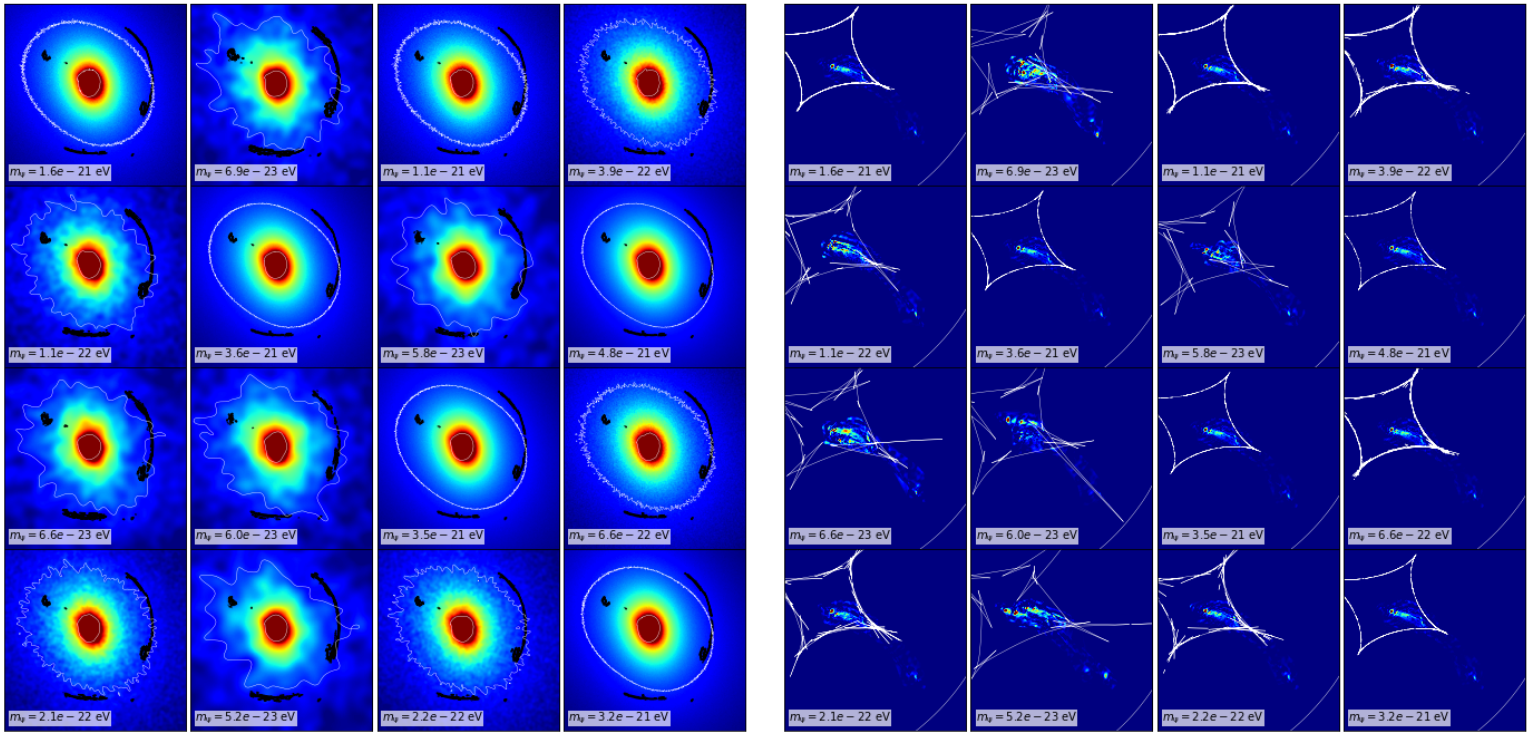

- Simple fuzzy lens model from Chan et al. (2020).
- In collaboration with Elisa Ferreira, Simon May, Jowett Chan, Simon White.
- Tentative lower bound of $M_\psi \gtrapprox 10^{-21}$ eV.

Sneak preview: Fuzzy DM

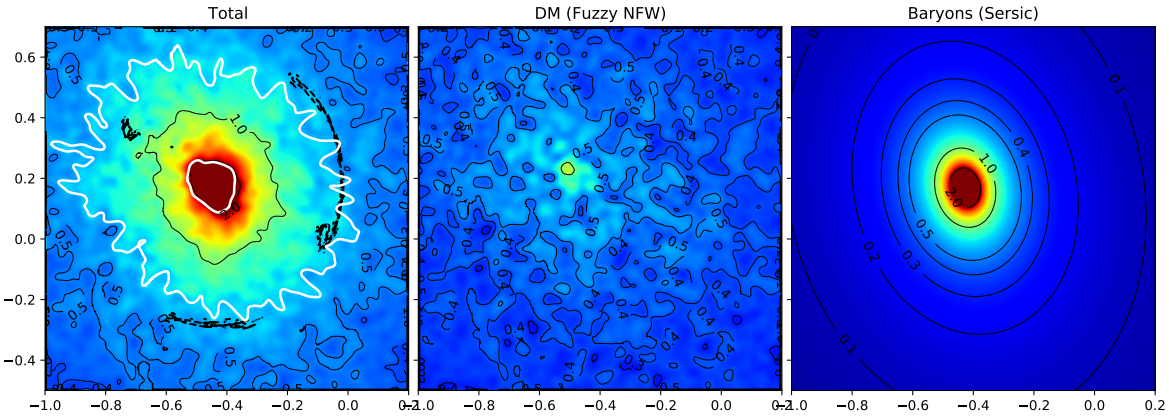

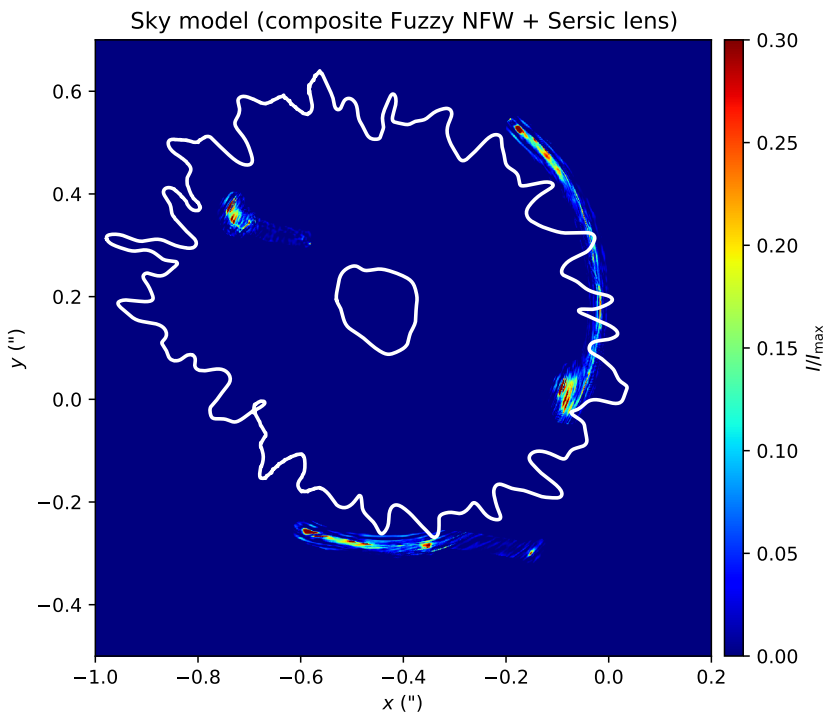

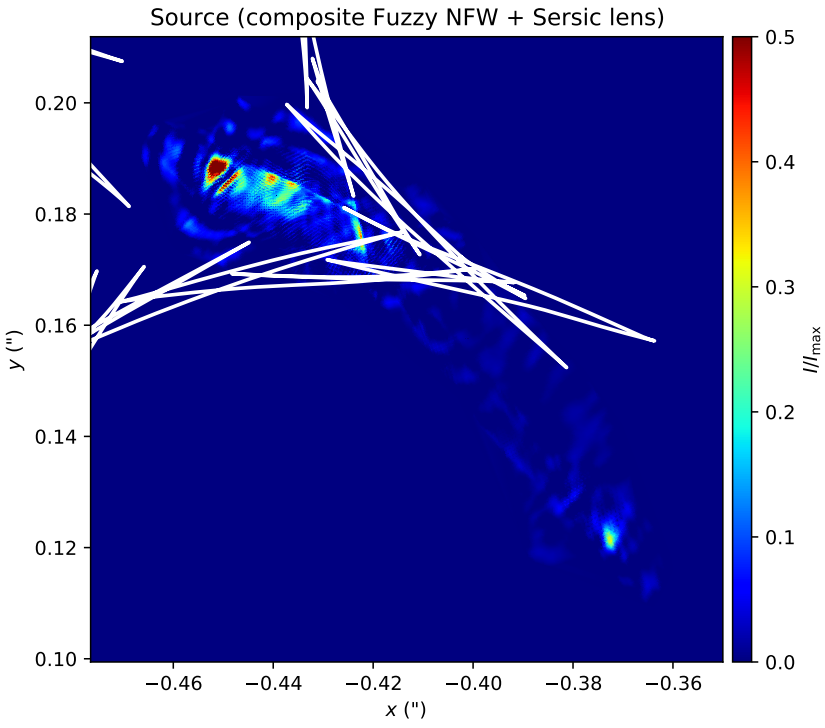

Bonus material

Evidence vs. regularization strength

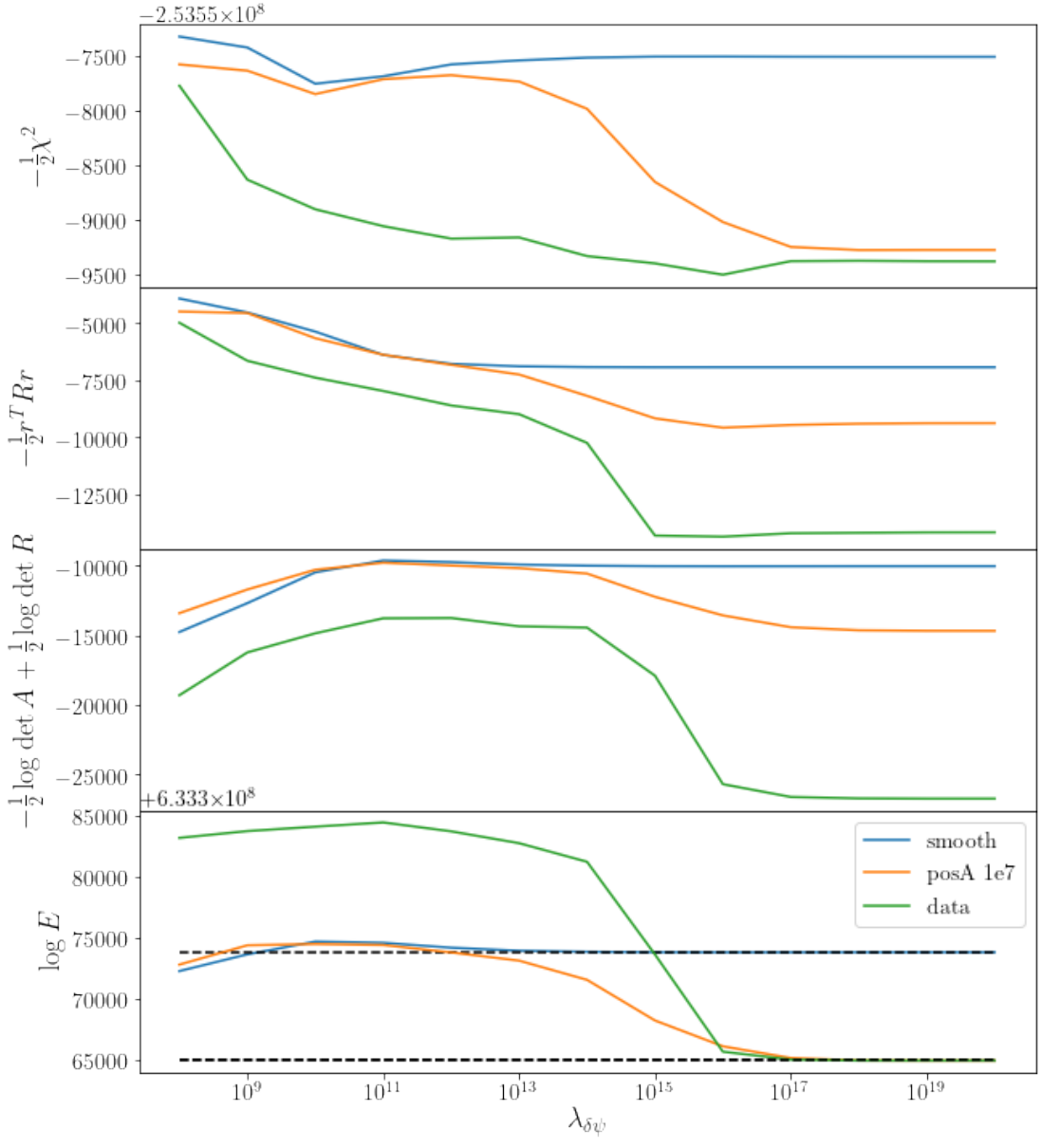

Self-calibration

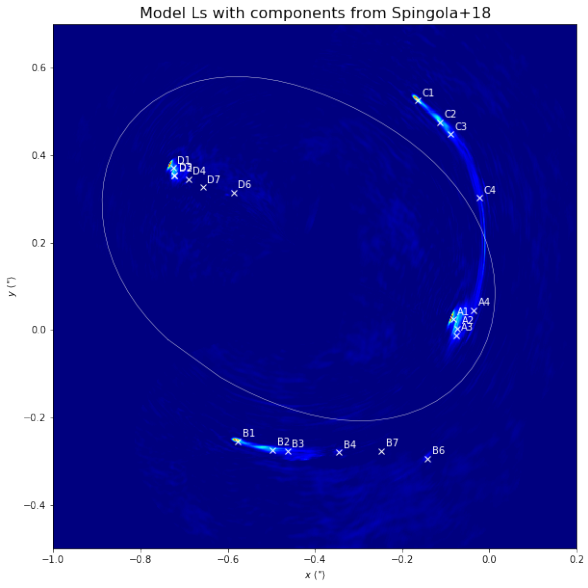

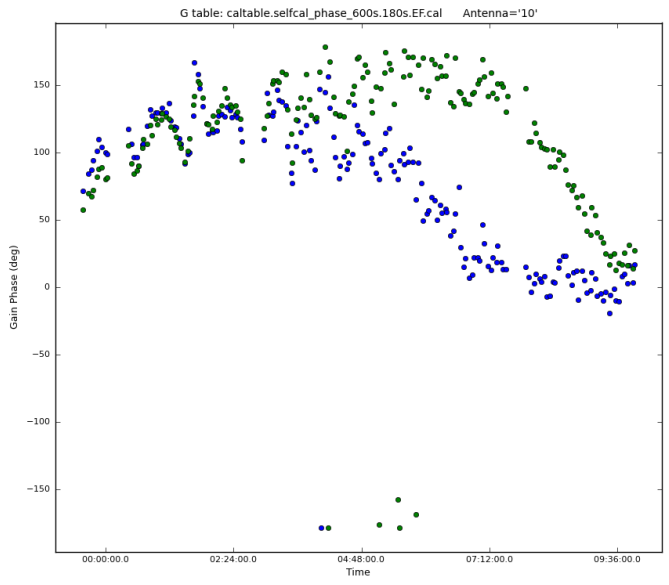

- Antenna-based phase errors can be corrected by fitting to a model image, re-fitting the model, and repeating as necessary
- We use the full lens modeling and source reconstruction to generate the model image (instead of e.g. CLEAN)
- A more elegant Bayesian approach would be nice in the future (e.g. Arras et al. 2019, or marginalizing over phase errors)

References

Birrer, S., Amara, A., and Refregier, A. (2017). Lensing substructure quantification in RXJ1131-1231: a 2 keV lower bound on dark matter thermal relic mass. *Journal of Cosmology and Astro-Particle Physics*, 2017(5):037.

Chan, J. H., Schive, H.-Y., Wong, S.-K., Chiueh, T., and Broadhurst, T. (2020). Multiple images and flux ratio anomaly of fuzzy gravitational lenses. *Physical Review Letters*, 125(11).

Chen, G. C. F., Suyu, S. H., Wong, K. C., Fassnacht, C. D., Chiueh, T., Halkola, A., Hu, I. S., Auger, M. W., Koopmans, L. V. E., Lagattuta, D. J., McKean, J. P., and Vegetti, S. (2016). SHARP - III. First use of adaptive-optics imaging to constrain cosmology with gravitational lens time delays. *MNRAS*, 462(4):3457–3475.

Courbin, F., Chantry, V., Revaz, Y., Sluse, D., Faure, C., Tewes, M., Eulaers, E., Koleva, M., Asfand iyarov, I., Dye, S., Magain, P., van Winckel, H., Coles, J., Saha, P., Ibrahimov, M., and Meylan, G. (2011). COSMOGRAIL: the COSmological MOnitoring of GRAvItational Lenses. IX. Time delays, lens dynamics and baryonic fraction in HE 0435-1223. *AAP*, 536:A53.

Despali, G. and Vegetti, S. (2017). The impact of baryonic physics on the subhalo mass function and implications for gravitational lensing. *MNRAS*, 469(2):1997–2010.

Despali, G., Vegetti, S., White, S. D. M., Giocoli, C., and van den Bosch, F. C. (2018). Modelling the line-of-sight contribution in substructure lensing. *MNRAS*, 475(4):5424–5442.

References ii

Fassnacht, C. D., Xanthopoulos, E., Koopmans, L. V. E., and Rusin, D. (2002). A Determination of H_0 with the CLASS Gravitational Lens B1608+656. III. A Significant Improvement in the Precision of the Time Delay Measurements. *ApJ*, 581(2):823–835.

Hezaveh, Y. D., Dalal, N., Marrone, D. P., Mao, Y.-Y., Morningstar, W., Wen, D., Bland ford, R. D., Carlstrom, J. E., Fassnacht, C. D., Holder, G. P., Kemball, A., Marshall, P. J., Murray, N., Perreault Levasseur, L., Vieira, J. D., and Wechsler, R. H. (2016). Detection of Lensing Substructure Using ALMA Observations of the Dusty Galaxy SDP.81. *ApJ*, 823:37.

Johnson, T. L., Sharon, K., Gladders, M. D., Rigby, J. R., Bayliss, M. B., Wuyts, E., Whitaker, K. E., Florian, M., and Murray, K. T. (2017). Star Formation at z = 2.481 in the Lensed Galaxy SDSS J1110 = 6459. I. Lens Modeling and Source Reconstruction. *ApJ*, 843(2):78.

Koopmans, L. V. E., Barnabe, M., Bolton, A., Bradac, M., Ciotti, L., Congdon, A., Czoske, O., Dye, S., Dutton, A., Elliasdottir, A., Evans, E., Fassnacht, C. D., Jackson, N., Keeton, C., Lasio, J., Moustakas, L., Meneghetti, M., Myers, S., Nipoti, C., Suyu, S., van de Ven, G., Vegetti, S., Wucknitz, O., and Zhao, H. S. (2009). Strong Gravitational Lensing as a Probe of Gravity, Dark-Matter and Super-Massive Black Holes. In *astro2010: The Astronomy and Astrophysics Decadal Survey*, volume 2010, page 159.

Leethochawalit, N., Jones, T. A., Ellis, R. S., Stark, D. P., Richard, J., Zitrin, A., and Auger, M. (2016). A Keck Adaptive Optics Survey of a Representative Sample of Gravitationally Lensed Star-forming Galaxies: High Spatial Resolution Studies of Kinematics and Metallicity Gradients. *ApJ*, 820(2):84.

Lovell, M. R., Frenk, C. S., Eke, V. R., Jenkins, A., Gao, L., and Theuns, T. (2014). The properties of warm dark matter haloes. *MNRAS*, 439(1):300–317.

Mao, S. A., Carilli, C., Gaensler, B. M., Wucknitz, O., Keeton, C., Basu, A., Beck, R., Kronberg, P. P., and Zweibel, E. (2017). Detection of microgauss coherent magnetic fields in a galaxy five billion years ago. *Nature Astronomy*, 1:621–626.

References iii

Powell, D., Vegetti, S., McKean, J. P., Spingola, C., Rizzo, F., and Stacey, H. R. (2021). A novel approach to visibility-space modelling of interferometric gravitational lens observations at high angular resolution. *MNRAS*, 501(1):515–530.

Ritondale, E., Vegetti, S., Despali, G., Auger, M. W., Koopmans, L. V. E., and McKean, J. P. (2019). Low-mass halo perturbations in strong gravitational lenses at redshift z 0.5 are consistent with CDM. *MNRAS*, 485(2):2179–2193.

Rizzo, F., Vegetti, S., Fraternali, F., and Di Teodoro, E. (2018). A novel 3D technique to study the kinematics of lensed galaxies. *MNRAS*, 481(4):5606–5629.

Rusu, C. E., Wong, K. C., Bonvin, V., Sluse, D., Suyu, S. H., Fassnacht, C. D., Chan, J. H. H., Hilbert, S., Auger, M. W., Sonnenfeld, A., Birrer, S., Courbin, F., Treu, T., Chen, G. C. F., Halkola, A., Koopmans, L. V. E., Marshall, P. J., and Shajib, A. J. (2019). H0LiCOW XII. Lens mass model of WFI2033-4723 and blind measurement of its time-delay distance and H_0. *arXiv e-prints*, page arXiv:1905.09338.

Spingola, C., McKean, J. P., Auger, M. W., Fassnacht, C. D., Koopmans, L. V. E., Lagattuta, D. J., and Vegetti, S. (2018). SHARP - V. Modelling gravitationally lensed radio arcs imaged with global VLBI observations. *MNRAS*, 478(4):4816–4829.

Spingola, C., McKean, J. P., Vegetti, S., Auger, M. W., Koopmans, L. V. E., Fassnacht, C. D., Lagattuta, D. J., Powell, D., Rizzo, F., Stacey, H. R., and Sweijen, F. (2019). SHARP $-$ VI. Evidence for CO (1$-$0) molecular gas extended on kpc-scales in AGN star forming galaxies at high redshift. *arXiv e-prints*, page arXiv:1905.06363.

Suyu, S. H., Chang, T.-C., Courbin, F., and Okumura, T. (2018). Cosmological Distance Indicators. *SSR*, 214(5):91.

References iv

Swinbank, A. M., Dye, S., Nightingale, J. W., Furlanetto, C., Smail, I., Cooray, A., Dannerbauer, H., Dunne, L., Eales, S., Gavazzi, R., Hunter, T., Ivison, R. J., Negrello, M., Oteo-Gomez, I., Smit, R., van der Werf, P., and Vlahakis, C. (2015). ALMA Resolves the Properties of Star-forming Regions in a Dense Gas Disk at z 3. *ApJ*, 806:L17.

Treu, T. and Marshall, P. J. (2016). Time delay cosmography. *AAPR*, 24(1):11.

Vegetti, S., Koopmans, L. V. E., Auger, M. W., Treu, T., and Bolton, A. S. (2014). Inference of the cold dark matter substructure mass function at z = 0.2 using strong gravitational lenses. *MNRAS*, 442(3):2017–2035.

Vegetti, S., Koopmans, L. V. E., Bolton, A., Treu, T., and Gavazzi, R. (2010). Detection of a dark substructure through gravitational imaging. *MNRAS*, 408(4):1969–1981.

Vegetti, S., Lagattuta, D. J., McKean, J. P., Auger, M. W., Fassnacht, C. D., and Koopmans, L. V. E. (2012). Gravitational detection of a low-mass dark satellite galaxy at cosmological distance. *Nature*, 481(7381):341–343.

Wong, K. C., Suyu, S. H., Auger, M. W., Bonvin, V., Courbin, F., Fassnacht, C. D., Halkola, A., Rusu, C. E., Sluse, D., Sonnenfeld, A. r., Treu, T., Collett, T. E., Hilbert, S., Koopmans, L. V. E., Marshall, P. J., and Rumbaugh, N. (2017). H0LiCOW - IV. Lens mass model of HE 0435-1223 and blind measurement of its time-delay distance for cosmology. *MNRAS*, 465(4):4895–4913.